

**SIGNIFICANT BUILDING RESPONSE RECORDS  
FROM THE 2011 TOHOKU EARTHQUAKE AND  
THE IMPLICATIONS FOR SEISMIC DESIGNS AND ANALYSES**

Kazuhiko Kasai and Kazuhiro Matsuda

Structural Engineering Research Center  
Tokyo Institute of Technology, Yokohama, JAPAN

**Abstract**

Many tall buildings in Tokyo metropolitan area were strongly shaken during the Tohoku Earthquake, March 11, 2011. Most of them are less than 40 years old, and experienced the shaking of such a strong level for the first time, although they suffered little damage. The buildings are conventional seismically-resistant buildings, and those constructed after the 1995 Kobe Earthquake are typically supplementally-damped buildings or base-isolated buildings for seismic damage reduction. Some of the tall buildings are instrumented with sensors and their motions recorded during the event. This paper discusses recorded responses of such tall buildings in Tokyo employing the three distinct structural systems. By estimating contributions of multiple vibration modes, various shaking phenomena observed in the tall building are clarified. Characteristics of the distinct systems and their effects on building contents are contrasted based on mode-based analyses.

**Introduction**

**The Tohoku Earthquake**

At 14:46 on March 11, 2011, the East Japan Earthquake of magnitude 9.0 occurred off Sanriku coast of Japan. It caused tremendous tsunami hazard in the pacific coast of eastern Japan, killing more than 15,000 people, destroying and washing away cities. The epicenter was 129km from Sendai, the largest city in the northeast of Japan. The depth of the hypocenter was 24 km. The recorded magnitude places the earthquake as the fourth largest in the world since 1900, following 1960 Chile Earthquake M9.5, 1964 Alaska Earthquake M9.2, 2004 Sumatra Earthquake M9.2, and it is the largest in Japan since modern instrumental recording began 130 years ago. The earthquake has recorded the seismic intensity 7, highest in the Japan Meteorological Agency scale, in the north of Miyagi prefecture.

There were many strong earthquake observation networks in operation under the management of research institutes, universities and companies. A large amount of data was well recorded during the earthquake. Figure 1 shows the distribution of peak ground acceleration (PGA) and velocity (PGV) recorded during the earthquake. K-NET Tsukidate, located in Kurihara city, Miyagi prefecture, is the only station that recorded Intensity 7 during the main shock. A maximum acceleration in the N-S direction reached almost  $2699 \text{ cm/s}^2$ , representing that the main shock caused excessively severe earthquake motions. Strong motions with PGA

larger than  $200 \text{ cm/s}^2$  were observed over a very wide area from Ibaraki to South Iwate. Tokyo is located 300 km away from the epicenter (Figure 1), and its stations recorded PGA of 50 to  $150 \text{ cm/s}^2$ . The records from stations close to epicenter, such as Sendai, show two wave groups with a time interval of about 50 seconds, and those from southern station such as Ibaraki and Tokyo areas show one large wave group. Such phenomenon occurred due to difference of focal rupture process and the wave propagation to recording stations in the northern and southern portions of the fault area of 500 km long.

As explained elsewhere (Kasai et al. 2012, 2013), many of the ground motion records in Tokyo showed the spectral velocity almost uniform for the vibration periods from 0.5s and 20s, and its magnitude exceeded even the largest spectral value due to the 2004 Niigata Chuetsu Earthquake that concentrated at the period about 7s. Thus, unlike the responses during the 2004 Niigata Chuetsu Earthquake, the responses of the tall buildings in Tokyo were dominated by not only the shorter period motions but also the long period motion.

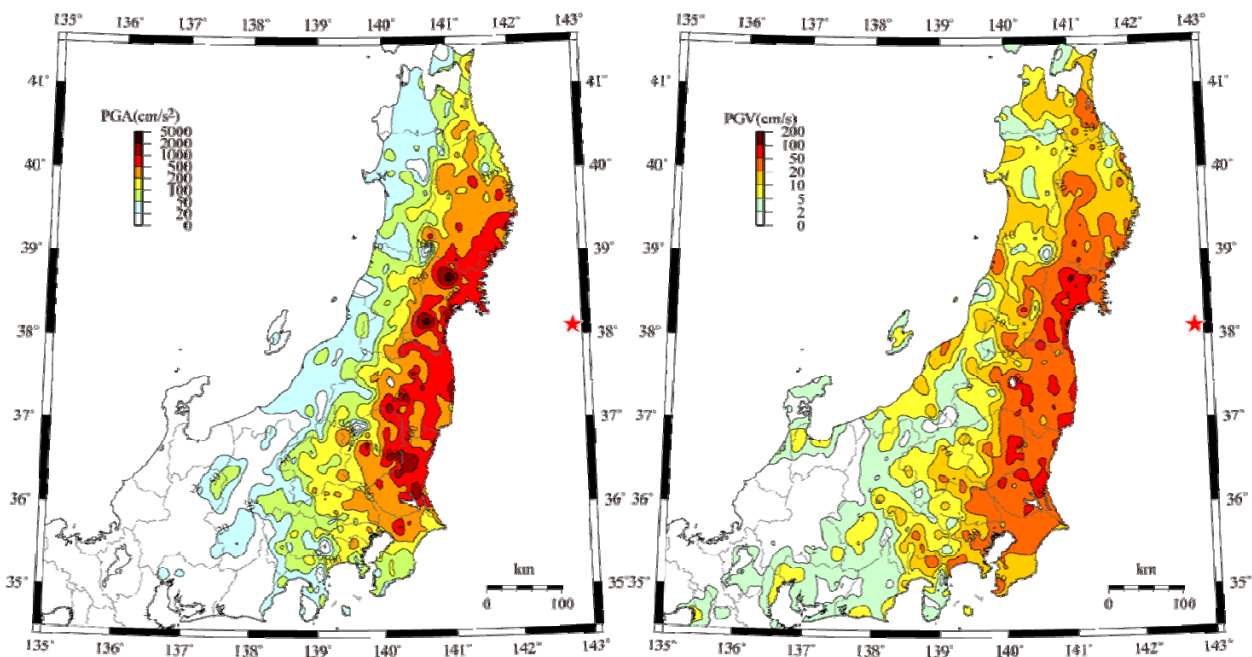


Figure 1. Peak ground accelerations and peak ground velocity recorded in eastern Japan during the 2011 Great East Japan Earthquake (From Dr. Kashima, Building Research Institute, [http://www.serc.titech.ac.jp/info/seminar/15WCEE\\_SS.html](http://www.serc.titech.ac.jp/info/seminar/15WCEE_SS.html))

## Objectives and Scopes

Where ground acceleration was large, except for some areas of soft ground, the response spectrum indicated short dominant period, which was probably the main reason for relatively small seismic damage. On the other hand, Tokyo relatively far from the epicenter was subjected to the ground motion of short to long period components. Many tall buildings have been constructed for the last 40 years in Tokyo, and the shaking they experienced is much stronger

than those in the past. Therefore, the response observed are believed to be the precursors for the performance of the tall buildings against the stronger shaking that will definitely occur in future.

Since some tall buildings were instrumented with accelerometers, acceleration records obtained during the earthquake would be one of the best resources to study the building responses (Kasai, 2011a). Pursuant to these, the objective of the present paper is to clarify behavior of tall buildings in Tokyo, based on the responses recorded during the 2011 Tohoku Earthquake. The paper will analyze acceleration records of a typical seismically-resistant building with a low damping ratio, and supplementally-damped and base-isolated buildings whose damping ratios are increased by the new technology using various types of dampers. Virtually, most Japanese tall buildings constructed after the 1995 Kobe Earthquake are either supplementally-damped or base-isolated in order to protect not only the human lives but also the structural components, nonstructural components, and building functions. Therefore, effectiveness of the new technology in achieving the above-mentioned performance will be discussed.

### **Buildings Considered and Data Analysis Schemes**

#### **Buildings Considered**

As the important reconnaissance effort of Japan Society of Seismic Isolation (JSSI), three investigation committees were established to examine performance of the buildings with three distinct systems (JSSI, 2012). Since little damage was found from most of such buildings, and available acceleration records of the buildings were studied and compared. This paper explains only a portion of the group of buildings studied by JSSI. The paper considers 29-story conventional seismic-resistant building, 21, 37, 38, 41, and 54-story supplementally-damped buildings, all located in Tokyo, and the 20-story base-isolated building in Yokohama.

Figure 2 shows the response spectra of the base acceleration records in both x- and y-directions and damping ratio 5% for nine buildings located in Tokyo. The response spectra have small coefficient of variation of about 0.2 at the middle to long period range. In view of the strong randomness of earthquake motions, the intensity and characteristics of these input earthquake motions may be considered as similar ones. Consequently, it is reasonable to use the average to represent the input earthquake level in this area. In one sense, it could be considered that all the nine buildings were subjected to a common ground shaking characterized by the average spectral plots.

The ratio of accelerations of top to base will be named as “acceleration magnification ratio (AMR)”. In Figure 3, its value is shown with respect to each building height. In addition to the nine buildings considered in Figure 2, twelve buildings (Kasai, 2011a) are added for comparison over wide range. As noted above, the response spectra for the buildings are similar, and the vibration period of the building is well correlated to its height. However, AMR in Figure 3 does not follow the trend of acceleration spectra in Figure 2a: It is very high for taller buildings, in contrast to low spectral accelerations in Fig. 2a (Kasai, 2011a,b). This is due to significant contribution of higher modes as well as low damping ratio in case of seismic-resistant buildings, as will be discussed.

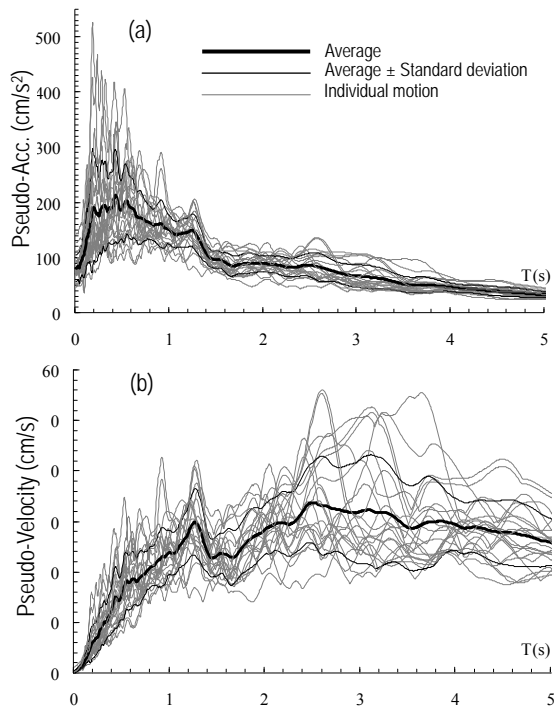


Figure 2. Response spectra ((a) to (c)) generated from the base motions of nine buildings (damping ratio 5%)

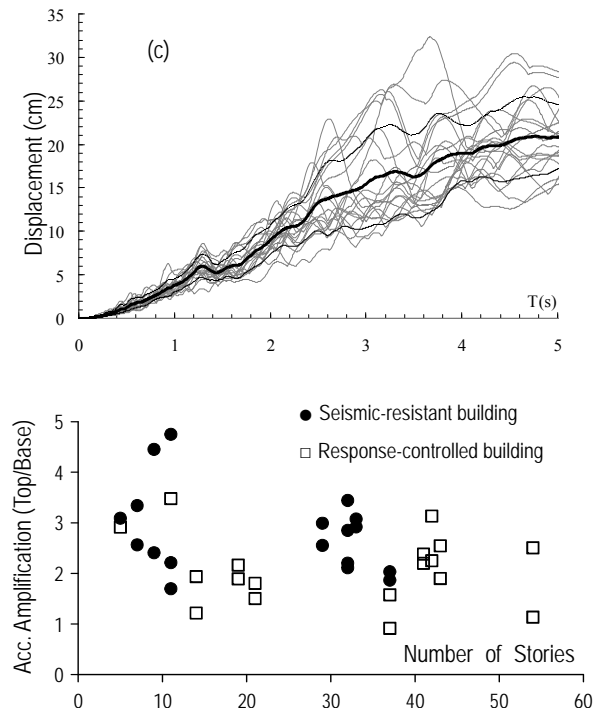


Figure 3. Acceleration magnification ratio (AMR) vs. number of stories of buildings

### Data Analysis by Standard Modal Approach

Displacements of the structure are calculated from the recorded accelerations by using two methods. The results are compared with each other in order to confirm their reliability (Kasai, 2013). Method 1 performs double integration together with hi-pass filtering in frequency domain. The cut-off frequency is typically 0.05 or 0.1Hz. Method 2 first obtains modal properties such as vibration period, damping ratio, and participation vector, by applying the basic system identification technique of fitting theoretical transfer function to the curve representing the spectral ratio of recorded accelerations. Using such modal properties and the base acceleration records, mode-superposition time history analysis is performed for the story where the sensor is located to obtain acceleration and displacement. The displacements are compared between methods 1 and 2, and accelerations from method 2 are compared with the recorded accelerations, and good match between them. Thus, calculated modal properties would be adequate and the buildings must also have behaved almost linearly.

Note that method 2 is based on the assumption of linear response, proportional damping, and real number mode. The agreement between the two methods suggests that the buildings had linear or slightly nonlinear behavior during the earthquake as well as moderate amount of damping.

Seismically-Resistant Building

Response Trends in Kanto Area

Six seismically resistant buildings investigated by JSSI and located in Kanto area were 8- to 37-story. The peak accelerations at the building base ranged from 49 to 210  $\text{cm/s}^2$ , and those at top of the building ranged from 150 to 427  $\text{cm/s}^2$ . The average story drift angle (ratio of peak displacement of top to its height) varied from 0.00061 to 0.00331 rad. In most tall buildings of steel construction, the damping ratios estimated were approximately in the range between 1% and 2%. This is believed to be a main reason for higher AMR shown in Figure 3. Excessive accelerations have been found to cause large economic loss due to the damage on non-structural components and facilities. Thus, acceleration magnification should be taken in structural design more seriously. By this reason, the following discussion will refer to both displacement and acceleration.

29-Story Building

The building is a seismically-resistant 29-story steel building constructed in 1989 (Hisada et al. 2011, 2012, Kasai et al. 2012). It is a school building of Kogakuin University, located in Shinjuku ward of central Tokyo. The building height is 143 m, structural framing height 127.8 m, and floor plan dimension is 38.4 and 25.6 m in EW and NS (x- and y-) directions, respectively (Hisada et al. 2011, 2012, Kasai et al. 2012).

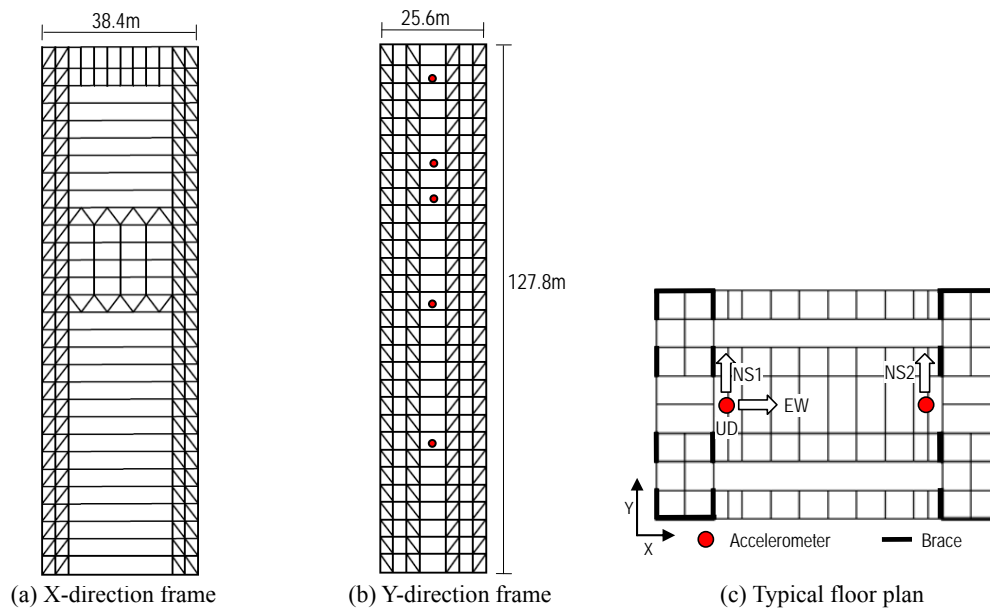


Figure 4. Seismically-resistant 29-story building

The peak accelerations in x- and y-directions were 91 and 89  $\text{cm/s}^2$  at the base, and 235 and 316  $\text{cm/s}^2$  at the top floor, respectively. The average drift angle is 0.029 rad., and the structure remained elastic. The vibration periods for the first three modes are 2.96s, 1.00s, and 0.52s for x-direction, and 3.10s, 0.94s, and 0.47s for y-direction, respectively. Likewise, damping ratios are 0.017, 0.018, and 0.034 for x-direction, and 0.021, 0.016, and 0.034 for y-direction,

respectively. Damping ratio 0.01 was estimated from small amplitude vibration tests before 2011 (Hisada 2011).

Figure 5a shows y-direction pseudo-acceleration response spectra  $S_{pa}$  of recorded building base accelerations (solid line) and that of recorded building top floor accelerations (broken line), respectively. Damping ratios are set to 2% and 3%, considering responses of building and non-structural component such as ceiling (Kasai 2011b), respectively. Similarly, Figure 5b shows displacement spectra  $S_d$ 's of the acceleration records, respectively. The two vertical axes on two sides of each figure are in reference to responses of the building and the component at the top floor, respectively.

$S_{pa}$ 's of recorded base acceleration are large at the building 2nd (0.94s) and 3rd (0.47s) mode periods, suggesting excitation of building's higher modes by ground shaking.  $S_{pa}$ 's of recorded top floor acceleration are extremely large at the 1st (3.09s) and 2nd (0.94s) modes of the building, and their values are 1,600 and 2,400  $\text{cm/s}^2$ , respectively. Time history analyses of components having the periods have indicated many cycles of large accelerations. On the other hand,  $S_d$ 's of both the building base and top floor accelerations almost monotonically increase with the period, suggesting strong dependency of displacement of both building and non-structural component at top floor on the 1st mode period (3.09s) of the building. Note that the broken line in Figure 5b shows the component may move 400cm, if it is flexible enough to resonate with the building's 1st mode. Figure 6 shows move of furniture and falling of ceiling and books due to the high accelerations. By these reasons, effects of the higher modes must be seriously considered when designing tall buildings.

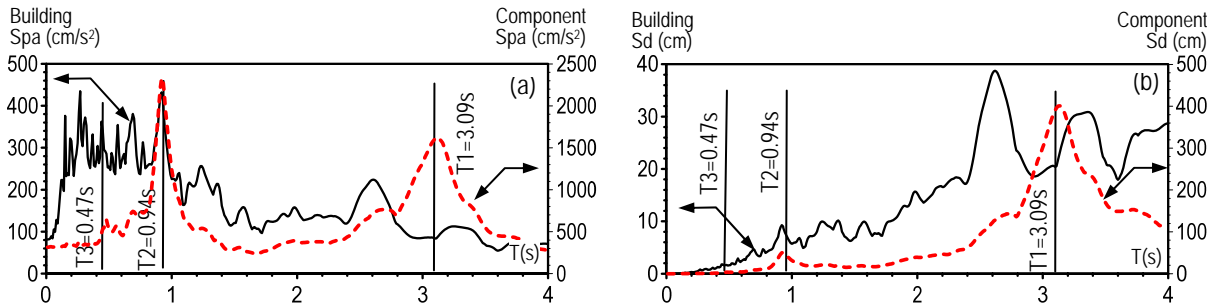
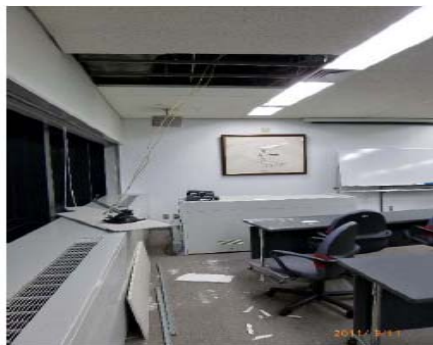


Figure 5. Response spectra (solid lines) of the building base acceleration, and those (broken lines) of the building top floor acceleration



(a) Falling of ceilings



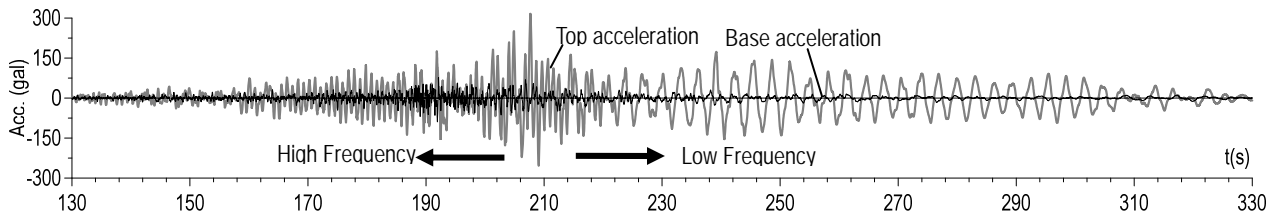
(b) Falling of books

Figure 6. Damage to contents of 29-story bldg. (From Prof. Hisada)

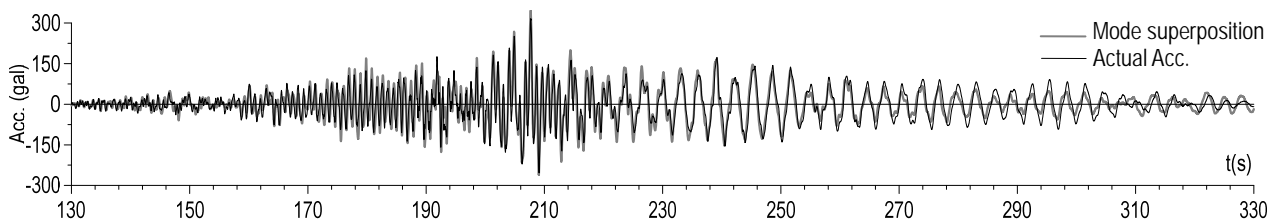
Figure 7a compares acceleration records at top floor and base in y-direction. The earthquake duration is long, and is considered to be about 200 seconds (Fig. 7a). For the first 90 seconds of the figure, high frequency response of the top floor is apparent, as confirmed by the large number of cycles per unit time. These are caused by the high-frequency ground shaking, as shown by the base accelerations. In contrast, for the last 110 seconds, low frequency response is dominant. The ground shaking is weak (Fig. 7a), but its low frequency contents excited the first mode and caused resonated response.

Figures 7b compares the top floor acceleration recorded with that calculated by method 2 mentioned earlier. The good agreement suggests that the mode method is effective, and the first three modes are adequate in response calculation for this case. Figure 7c compares relative displacement of top floor obtained by double integration of the record (method 1) with that calculated by method 2. In some cycles the peak values by the both method differ a little, but the displacements agree well overall.

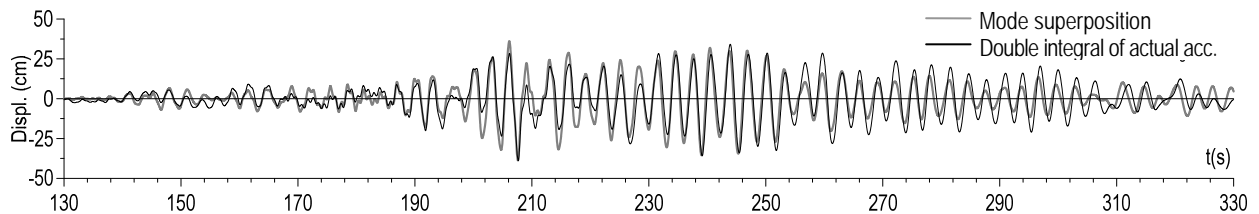
As is known, the contribution of each vibration mode depends on the type of response as well as the story level determining participation vector. Since the properties and responses of each vibration mode have been obtained, it is possible to discuss such contributions:



(a) Accelerations recorded at top and base.



(b) Comparison: acceleration obtained by mode superposition vs. actual recorded acceleration.



(c) Comparison: dispt. obtained by mode superposition vs. dispt. from double integral of recorded acceleration.

Figure 7. Acceleration records and accuracy of mode superposition method.

Figure 8a shows the acceleration of each mode at the top floor. As mentioned earlier, it is dominated by the 2nd, 1st, and 3rd modes in the order of weight for the first 90 seconds. For the later 110 seconds, the 1st mode response increases and become dominant, with slight contribution from the 2nd mode. As Figure 8b shows, for the 16th floor the 2nd mode is much more dominant, developing almost the same acceleration as top floor. As for the displacement at top floor (Fig. 8c), the 1st mode dominates throughout the entire duration.

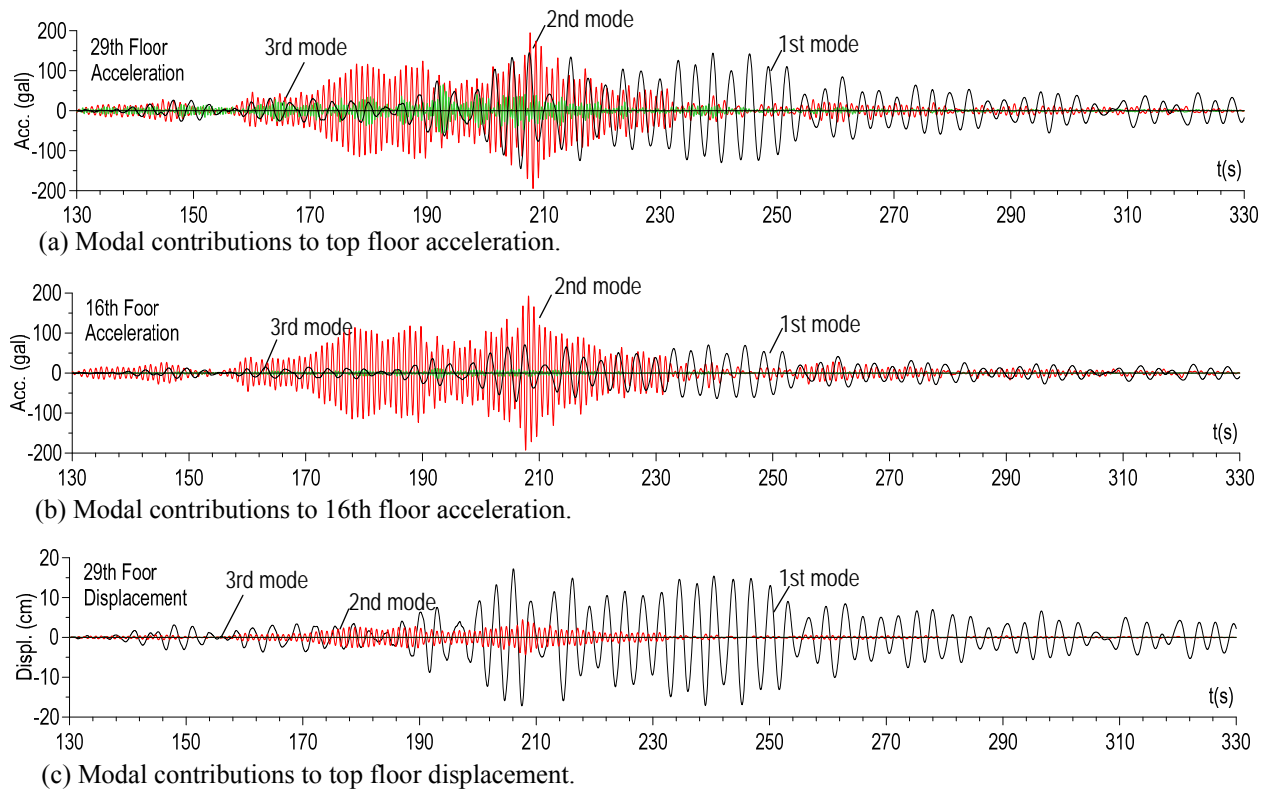


Figure 8. Contributions of the first three modes to acceleration and displacement of Building 1.

### Supplementally-Damped Buildings

#### Response Trends in Kanto Area: Deformation- & Velocity-Dependent Dampers

Ten supplementally-damped buildings investigated by JSSI and located in Kanto area were 5- to 54-Story. Peak accelerations at the building base ranged from 53 to 142  $\text{cm/s}^2$ , and those at top of the building ranged from 118 to 435  $\text{cm/s}^2$ . The average story drift angle varied from 0.00026 to 0.00372 rad. Note that the buildings with steel dampers showed high accelerations at top, similarly to the seismically-resistant buildings explained earlier. This is because the steel dampers were elastic or barely yielding for the level of the ground shaking in Tokyo, and dissipated little energy.

As a matter of fact, the above-mentioned difference among the deformation-dependent steel damper and three types of velocity dampers, oil dampers, viscous dampers, and viscoelastic dampers, respectively, were demonstrated by the full-scale tests of 5-story supplementally

damped building using the world’s largest shake table called E-Defense (Kasai et al. 2009, Kasai 2013). Figure 9 depicts the hysteresis of the four damper types under minor, moderate, and major shaking. The steel damper is elastic at the minor shaking and did not dissipate seismic energy, whereas the three velocity-dependent dampers do even under small deformation. The force of the steel damper was also larger than others. These lead to larger accelerations of the building under minor to moderate shaking.

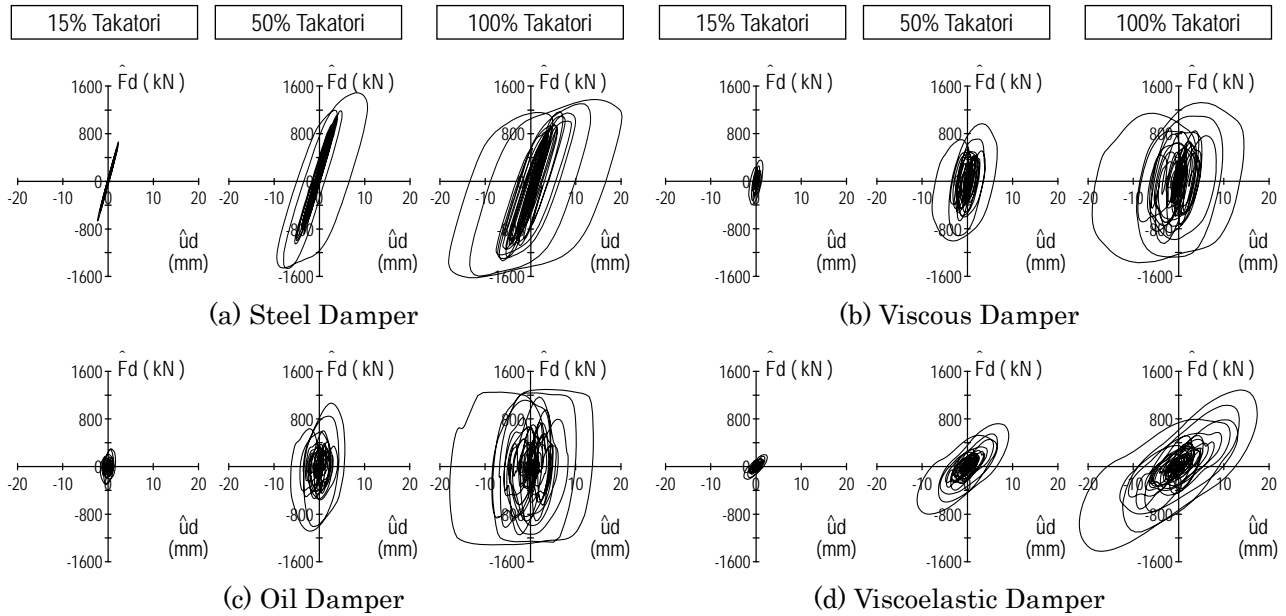
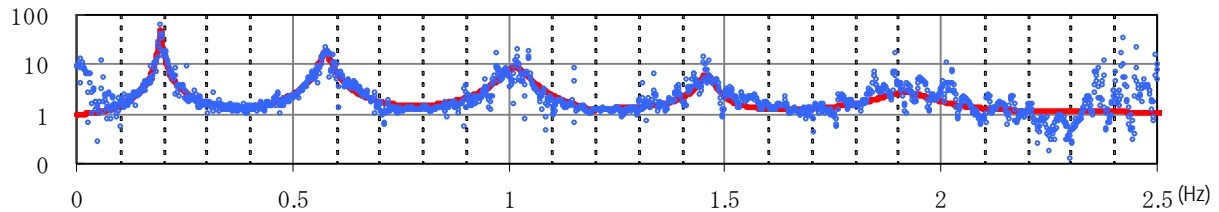


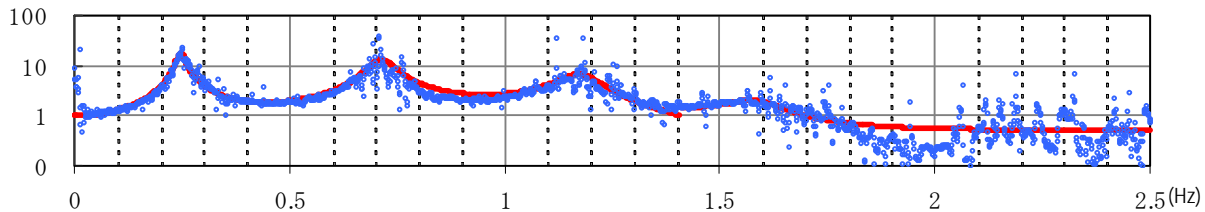
Figure 9 - Damper axial force and stroke, four types of dampers in the full-scale 5-story building tested by the world’s largest shake table (used 15, 50, and 100% scale ground accelerations recorded at the JR Takatori station during the 1995 Kobe earthquake)

In Japanese practice to-date, design criteria for supplementally-damped buildings have been set for displacement control, and rarely for acceleration control. The acceleration-induced hazard, however, appeared to be significant during the 2011 Tohoku earthquake, and its mitigation by adding damping seems essential. Therefore, adding velocity-dependent dampers capable of energy dissipation at small to moderate shaking would increase damping ratio.

The observations from the full-scale tests of the 5-story building (Figure 9) appear to be consistent with those of existing tall buildings with dampers. Figure 10 shows the transfer function obtained using the acceleration of building top floor and base for the 38-story building having steel dampers only (Fig. 10a), and the building having both steel dampers and viscous dampers (Fig. 10b). They are located nearby, and were subjected to almost the same ground shaking. The former shows the 1st mode damping ratio of 0.017, similar to the value obtained from the 29-story conventional building explained in the previous section. On the other hand, the latter showed the 1st mode damping ratio of 0.046. The larger damping ratio of the building with steel and viscous dampers can be understood from wider resonance curves (Figs. 10a, b). The damping ratio of 0.046 may not sound very high, but the amount of dampers and viscosity coefficients added are considerable, and still show good vibration control, as will be demonstrated in the subsequent sections.



(a) 38-story bldg. (179m) with steel dampers only, 1st mode damping ratio = 0.017, period = 5.08 s



(b) 37-story bldg. (198m) with steel & viscous dampers, 1st mode damping ratio = 0.046, period = 4.05 s

Figure 10 Transfer Functions of Tall Buildings (a) with Steel Dampers Only, and (b) with Steel and Viscous Dampers

### 21-, 41-, and 54-Story Buildings

Three tall buildings with velocity-dependent dampers will be discussed. They are 21-, 41-, and 54-story buildings as shown in Fig. 11. The first building is a 21-story government office building (Koyoma and Kashima 2011, Kasai 2011a, b, Kasai et al. 2012). It consists of a steel frame and 336 low yield point steel (wall) dampers and 284 viscous (wall) dampers (Fig. 11a). As found from the full-scale test mentioned earlier, a contrasting case of using only steel dampers lead to large accelerations, since the dampers remained elastic for the level of shaking in Tokyo (Kasai 2011a,b, Kasai et al. 2012). The 21-story building had been designed to avoid such a situation, expecting that viscous damper would dissipate energy from a small earthquake, and steel damper, the most economical among all types, would dissipate considerable amount of energy at a large quake, respectively.

The second building is a 41-story office building (Kasai 2011a,b, Kasai et al. 2012). It consists of a frame using concrete-filled tube columns and steel beams, and 688 oil dampers (Fig. 11b) mentioned earlier. The relief mechanism to limit the force was provided, but most likely relief did not occur for the level of shaking.

The third building is a 54-story office steel building constructed in 1979. It was retrofitted in 2009 (Maseki et al. 2011, Kasai et al. 2011a,b) by attaching 288 oil dampers (Fig. 11c). 12 dampers per floor were attached to middle 24 stories of the building. The oil damper is similar to those used for the 41-story building, except that its relief mechanism is modified to reduce forces near peak responses. This aims to reduce the axial force of the column transmitting the damper force, and consequently uplift force of foundation. Most likely, however, the relief did not occur for the level of shaking.

The acceleration magnification ratio (AMR), the largest ratio of both x- and y-directions, was 1.80, 2.38, and 2.51 for the 21, 41, and 54-story buildings, respectively. They are well

below the ratio of 3.55 obtained in the seismically-resistant 29-story building. The three buildings remained elastic, and modal properties are obtained from method 2, and estimated 1st mode damping ratios are about 4%, and those of the 2nd and 3rd modes are almost equal or larger. The 1st mode vibration periods in x- and y-directions are 1.83s and 1.97s for the 21-story building, 3.97s and 4.10s for the 41-story building, and 5.37s and 6.43s for the 54-story building..

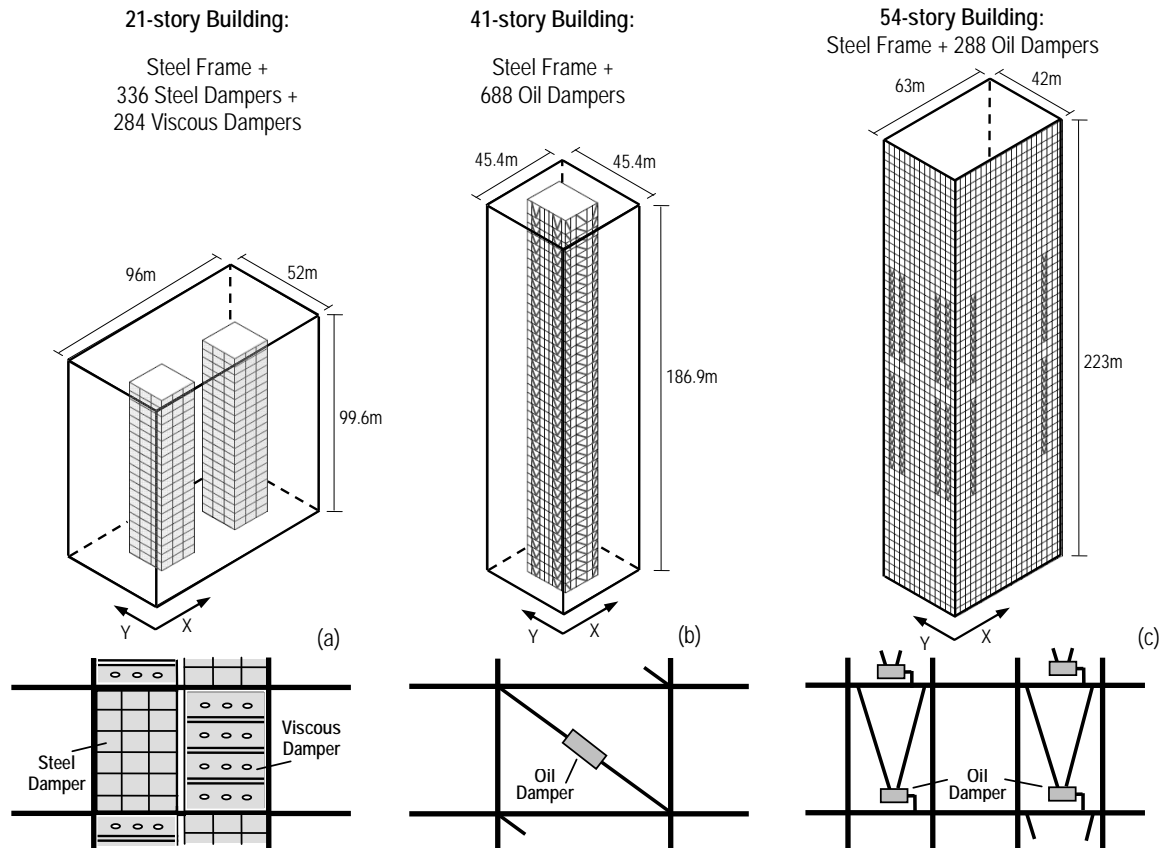


Figure 11 Three buildings with velocity-dependent dampers.

Modal properties were estimated for the three buildings, and their accelerations and displacements are obtained from superposition up to the 3rd mode, and accuracies are confirmed to be even better than those shown in Figs. 7b and c shown earlier. Such responses at top floor are shown by black lines in Figures 12, 13, and 14 for 21-, 41- and 54-story buildings, respectively. In these three buildings, the acceleration is dominated by the 2nd and 3rd modes for about 100 seconds, and by the 1st mode for later 200 seconds. Whereas, the displacement is dominated by the 1st mode throughout the shaking.

This trend is like that of seismically-resistant 29-story building (Fig. 8), but the amplitudes are believed to be smaller due to the supplemental damping. Thus, the responses are compared with those of lower but possible damping ratio representing a hypothetical case of not using the dampers. The modal period is unchanged, assuming small stiffness of the damper. The 1st to 3rd mode damping ratios are uniformly set to 1% and superposition is repeated. The results are shown by gray lines in Figs. 12, 13, and 14 for 21-, 41- and 54-story buildings, respectively.

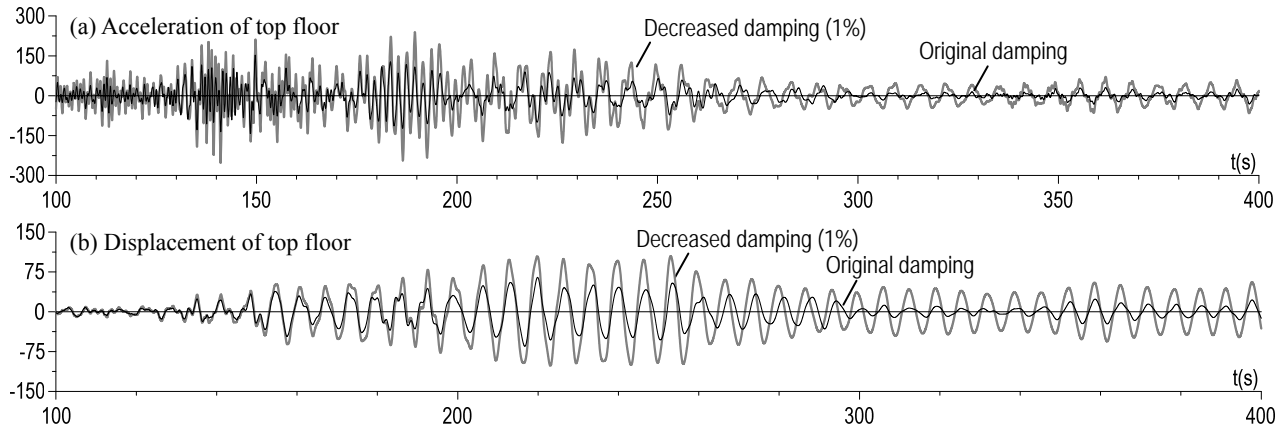


Figure 12. 21-story bldg. responses with original and lowered damping ratios (y-dir.).

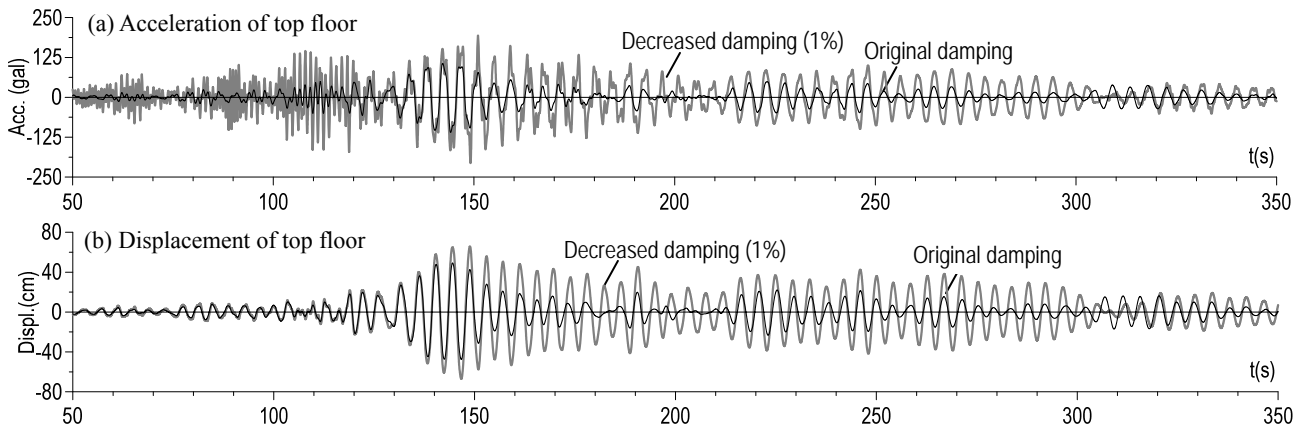


Figure 13. 41-story bldg. responses with original and lowered damping ratios (x-dir.).

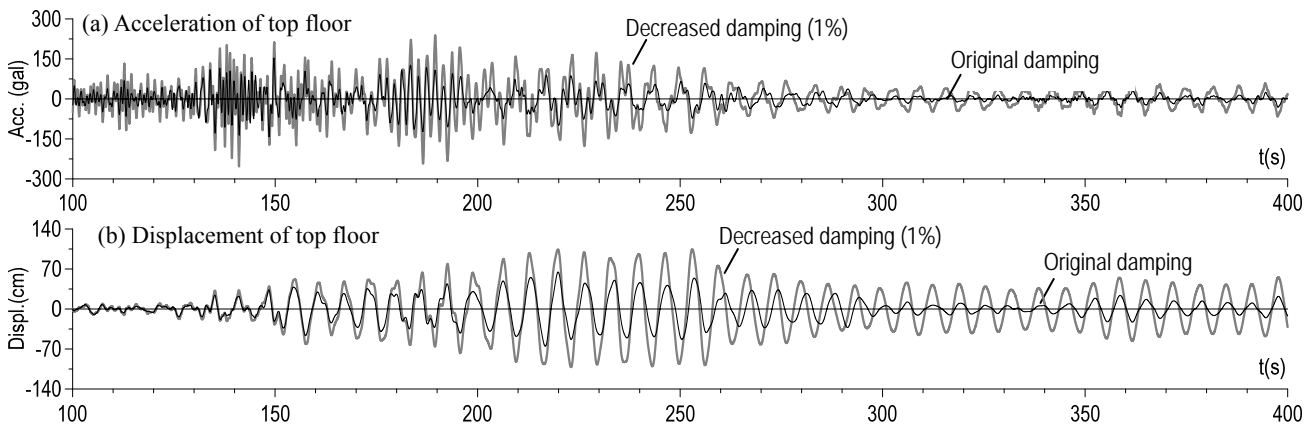


Figure 14. 54-story bldg. responses with original and lowered damping ratios (y-dir.).

In all the three buildings, their responses are considerably smaller (black lines) than those with lowered damping (gray line). The peak accelerations and displacements are about 0.5 and 0.7 times those of the low damping case. Moreover, between significant ground shakings, the

responses decay much faster, and number of large cycles is reduced considerably. These help reducing damage and fatigue of structural and non-structural component as well as fear or discomfort of the occupants. In order to quantify such an effect, root mean square of the acceleration and displacement at top are calculated, and their values appear to be about 0.4 and 0.5 times those with low damping, respectively.

### Base-Isolated Buildings

#### Response Trends in Kanto Area

Sixteen base-isolated buildings investigated by JSSI and located in Kanto area are 2- to 21-Story. About 60% of the buildings use natural rubber bearings with dampers, which is consistent with the nationwide trend in Japan. And, about 40% of the buildings use high damping rubber bearing or lead rubber bearing, without utilizing externally attached dampers. Peak accelerations at the ground level ranged from 45 to 402  $\text{cm/s}^2$ , and those at top of the building ranged from 57 to 181  $\text{cm/s}^2$ . The maximum displacement at the isolation level, typically estimated from the accelerations and their double integrations, ranged from 59 to 140 mm.

As shown in Figure 15, the acceleration magnification ratio (AMR), is estimated for each horizontal direction and each building, and it is plotted against the PGA (Kasai et al. 2013). Remarkably, AMR and PGA are strongly correlated, and AMR becomes smaller for the larger PGA. The hysteretic characteristic of the base-isolated level is typically a softening type, in which larger excitation results in more deformation, less equivalent stiffness and more energy dissipation, leading to a high damping system. In such a case, better control of accelerations occurs, reducing the AMR. This will be further discussed in a later section by referring to such hysteresis behavior.

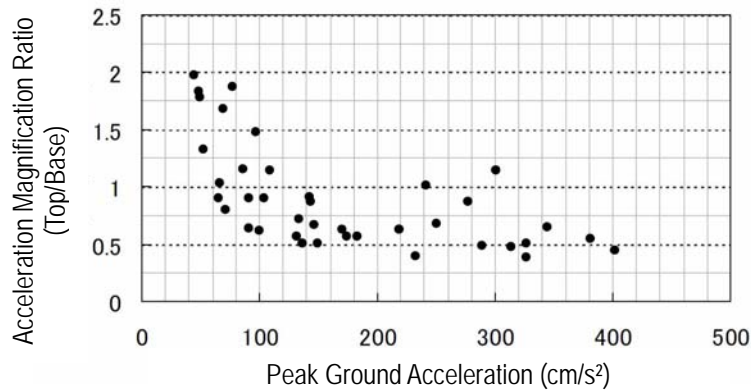


Figure 15. Relationship between acceleration magnification ratio (AMR) and peak ground acceleration (PGA) of base-isolated buildings

#### 20-Story Isolated Building

Figure 16 shows the 20-story base-isolated building of Tokyo Institute of Technology located in Yokohama, Kanagawa Prefecture (Matsuda et al. 2012). The foundation and 1st floor of this building are RC structure, and other floors are hybrid with steel beams and CFT columns. Figure 17 shows the plan of the isolation floor and isolation system: the 1,200 mm diameter rubber bearing with conical spring (Fig. 17a) is installed in position A. Combined steel damper

and 1,100 mm diameter rubber bearing (Fig. 17b) and steel damper alone (Fig. 17c) are installed in positions C and D, respectively. In position E, the 1,000kN oil damper (Fig. 17e) is installed.

The so-called mega-braces ( $\square$  - 500mm x 160mm x 19 to 32mm) on both sides of the building stiffen the superstructure. Because of high aspect ratio of 5 (Fig. 16), large uplift force may develop at the rubber bearings due to the large overturning moment. To avoid this, the bearings are allowed to move upward within 20 mm of gap distance (Fig 17a).

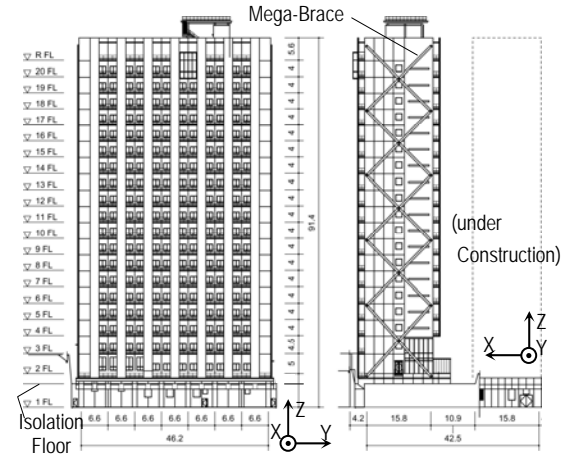


Figure 16 Base-isolated 20-story building (unit: m)

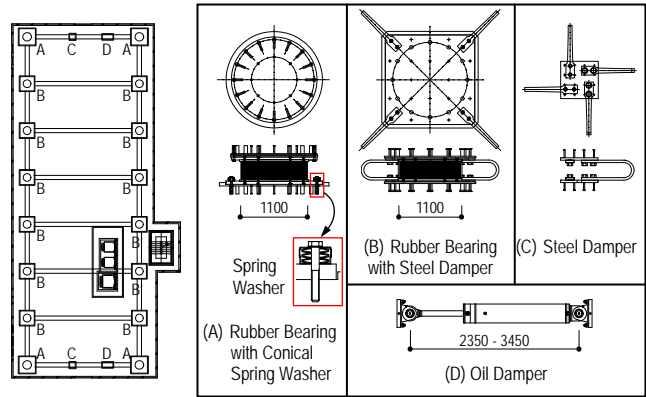


Figure 17 Isolated floor and isolation system

Figure 18 compares the deformations of isolation system obtained from the scratched lines created by the trace recorders, data from wire type displacement sensors, and double integration of the relative acceleration measured by the sensors above and below the isolation system. The deformations obtained from the three distinct methods agree well, validating the measurement method and data. Peak deformations of 69 and 91mm are recorded in X- and Y-directions, respectively, and torsional response appears to be negligible because the two results at the two most remote points are identical (Figs. 18a and b).

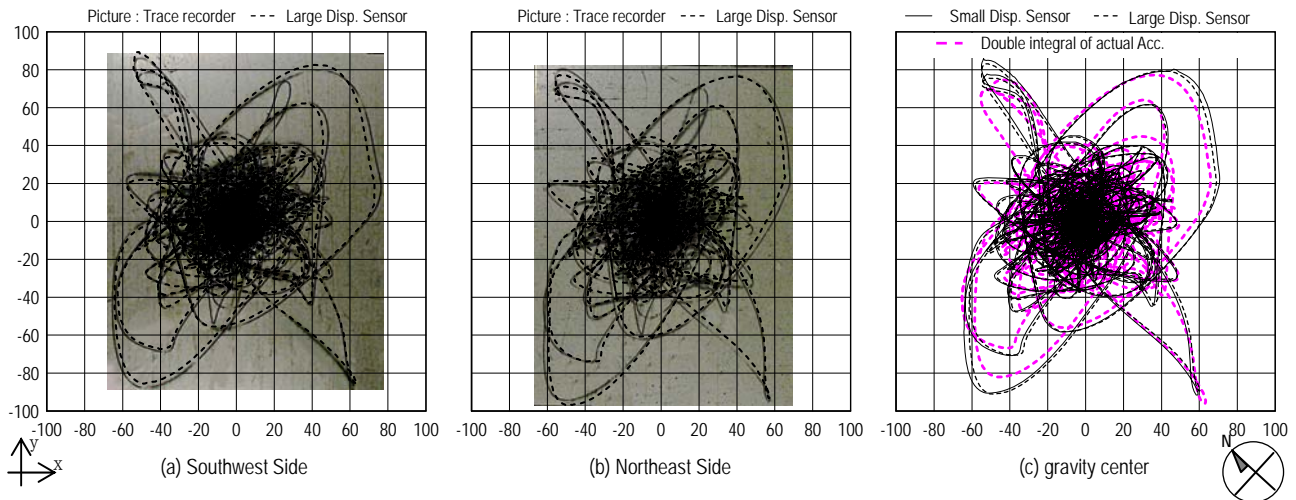


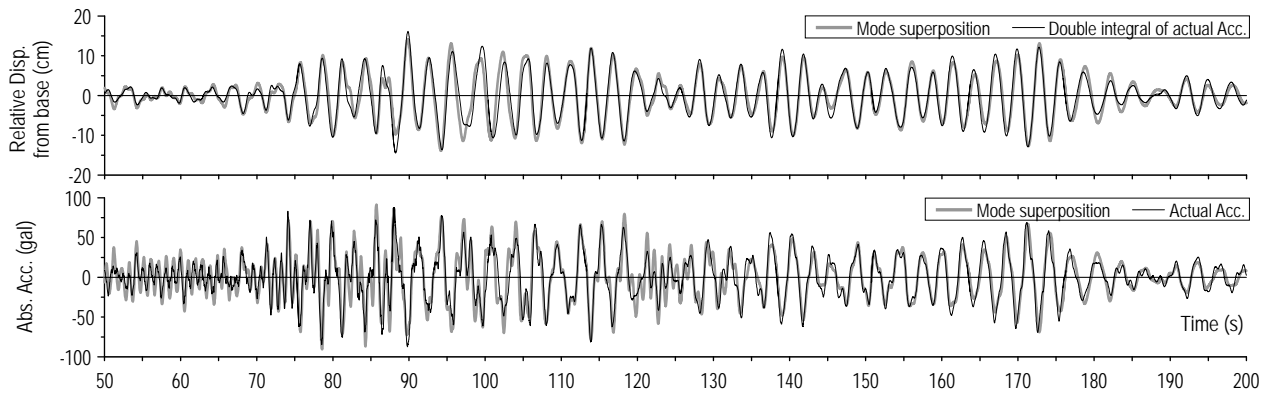
Figure 18. Isolation system deformations : recorded by the three different methods (Unit : mm)

Because the whole structure is a non-proportional damping system having high damping concentrated at the isolation floor, the data analysis method 2 discussed earlier is used in two different cases as described below:

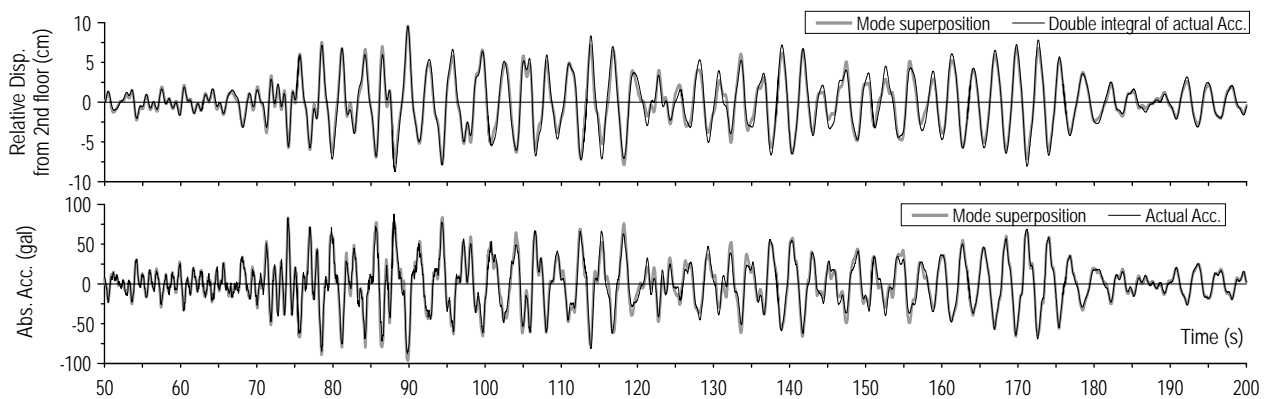
- (1) Like the proportional damping case, modal period, damping ratio, and participation vector are obtained by the basic system ID technique using the acceleration of ground (1st) level as input and those of other (2nd, 7th, 14th, and 20th) levels as output for the transfer function.
  - (2) The system ID is applied to superstructure only, using the acceleration of the base (2nd) level as input and those of other (7th, 14th, and 20th) levels as output for the transfer function.
- The properties up to the third mode were estimated for the above two cases. The first mode properties are listed in Table 1.

Table 1. Base-isolated 20-story building: the first mode vibration periods and damping ratios estimated for cases (1) and (2), respectively.

	X-direction		Y-direction	
	Period (s)	Damping ratio	Period (s)	Damping ratio
Base-isolated case (total building)	2.92	0.070	2.98	0.105
Seismic resitant case (only superstructure)	2.01	0.021	2.15	0.046



(a) Case 1: Analysis of whole structure (isolation system included), using 1st floor accelerations as input.



(b) Case 2: Analysis of superstructure only, using 2nd floor accelerations as input.

Figure 19. Comparison of top-level behavior between recorded data and modal analysis using identified modal frequencies and damping ratios in X-direction

Figure 19 compares the building top level displacements and accelerations between the records and mode superposition analysis results. The latter used the modal properties estimated from the basic system ID technique explained above. Even for the non-proportional case (Case (1)), the analysis simulated well the time histories of displacement and acceleration (Fig. 19a). This is because yielding and hysteretic damping of the steel damper was not significant for the level of the deformations noted (Fig. 18). Since yield displacement of the damper is 32 mm, the ductility ratios in X- and Y-directions were only about 2 and 3, respectively. Another reason is that the flexible and tall superstructure contributes more to the displacement and acceleration at the top level, and it is closer to proportional damping system. Therefore, cases of shorter isolated building or significant yielding of damper would produce more errors than reported here. On the other hand, small damping and approximately proportional case (Case (2)) is simulated extremely well (Fig. 19b).

In addition to the mode-superposition time history analyses, more detailed system ID technique called the autoregressive with exogenous inputs (ARX) method (Isermann and Münchhof, 2011) is used to validate the modal properties of the whole building (e.g., Case (1) of Table 1). ARX method gives step-by-step estimate for damping ratio and vibration period, and the average taken between their highest and lowest values over the entire duration seems to agree with the value in Table 1 (Matsuda et al. 2012). Note also that the above methods consistently indicated larger period shift and damping ratio in Y-direction where dampers were yielding more.

**Additional Comments on Performance**

Based on validations described above, the vibration periods and damping ratios of Case (1) are estimated for the past records from (a) microtremor, (b) March 9 earthquake, (c) March 11 Tohoku Earthquake, (d) March 11 after-shock, and (e) microtremor. The ground motions of (b) and (d) are almost half of the ground motion (c), and the results are shown in Figure 20. It clearly indicates higher damping and longer period for the stronger ground shaking. Therefore, larger isolation effect from the steel dampers could be expected for stronger earthquake.

Note also that the acceleration magnification ratio (AMR) during the March 11 event was about 1.7 (Fig 21), and it was as high as 3.1 for the weaker ground motion considered above. The high-rise base-isolated building whose superstructure is relatively flexible (see Table 1) and the steel damper showing only moderate yielding made equivalent stiffness of the isolation

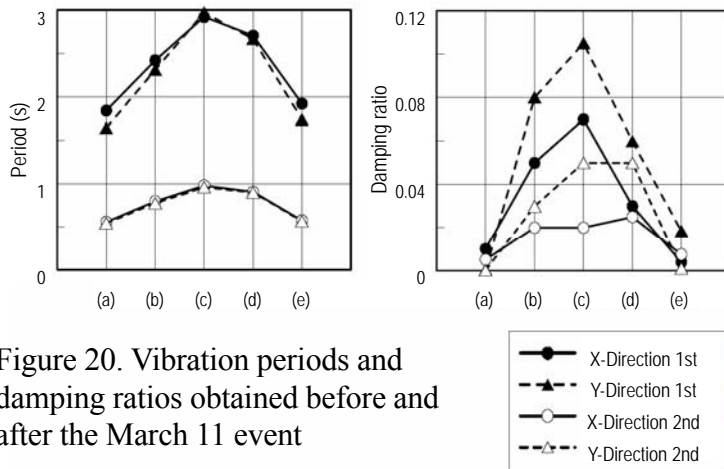


Figure 20. Vibration periods and damping ratios obtained before and after the March 11 event

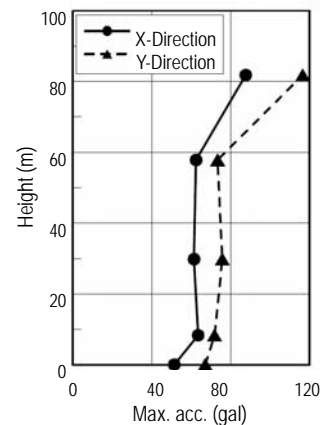


Figure 21. Peak accelerations

system relatively high, causing the building to behave like a seismically-resistant building. However, as noted above the performance is expected to be better from the stronger ground motions. This point, however, should be carefully examined considering much stronger earthquake that will definitely happen in the near future.

Like the supplementally-damped building cases discussed earlier, observed performance of the base-isolated building will be compared with that of the building without isolation system. The latter uses modal properties of the superstructure (Case (2)) and the ground (1st) level acceleration rather than the base (2nd) level accelerations that were used for the system ID. The result is shown in Figure 22. Although the displacements of the top level are similar in the two buildings, acceleration of the base-isolated building is only about 0.5 times that of the seismically-resistant building.

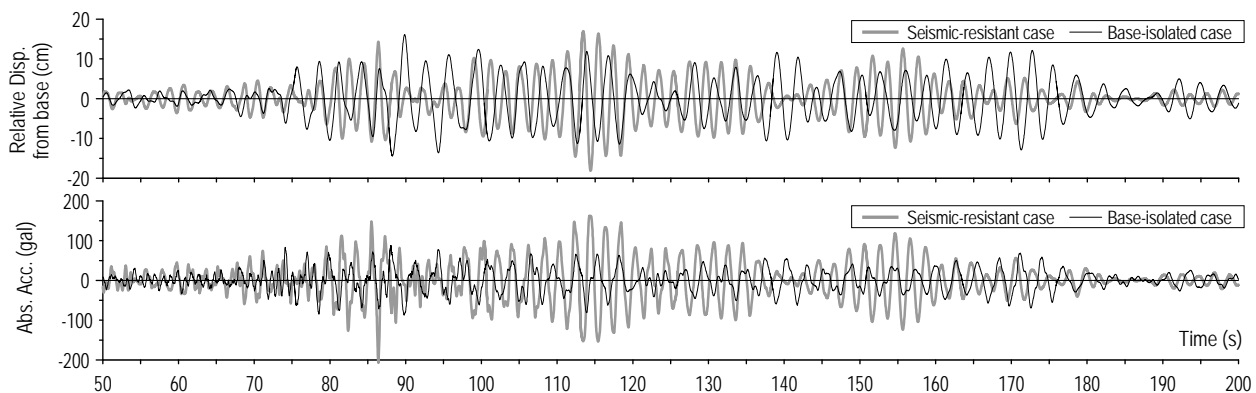


Figure 22. Comparison of base-isolated case and seismically-resistant case by modal analysis

As can be understood from this paper, the writers have been performing data analysis mainly by using the standard modal approach in various ways. However, for some cases of highly concentrated damping and/or nonlinearity in the building, floor-by-floor stick model or member-by-member frame model can provide different and useful information. The most significant advantage of such modeling is direct referencing to the physical responses rather than modal responses. The forces of a particular floor level or member are directly estimated by this model, which has been utilized to interpret the records at Tokyo Institute of Technology.

Figure 23 shows an example for such a model created to clarify the hysteretic responses and properties of the isolation system in the base-isolated 20-story building. Base shear and isolation system deformation are obtained by estimating inertia forces as well as the deformation from the recorded accelerations. The hysteresis is shown for three distinct phases of excitation, and linear and bilinear performance of the steel damper is clearly seen. The envelope curves are in excellent agreement with the design curves, therefore the steel damper has functioned as planned.

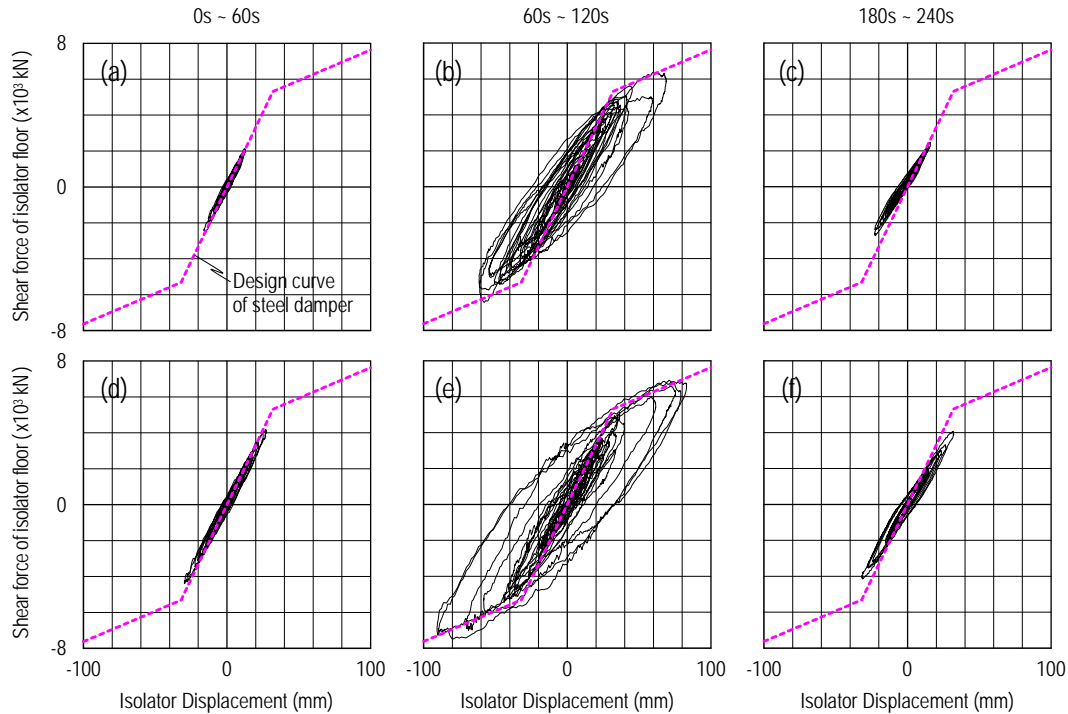


Figure 23. Hysteresis of isolation system in X-direction ((a) ~ (c)), and Y-direction ((d) ~ (f))

### Accelerations of Nonstructural Components

Inertia forces against structural and non-structural components including equipment and building content are produced by accelerations in the building. Large accelerations typically developed at upper stories cause falling, overturning, shifting, crashing, rapture, and excessive vibration of a variety of non-structural components. Economic loss due to damage of non-structural components is much more than that of structural damage. Falling of ceilings and other components may also cause death of occupants. Such failures due to the 2011 Tohoku Earthquake were enormous.

Figure 24a-d show component acceleration spectra (CAS) for the top floors of the 29-story seismically-resistant building, and 21, 41, and 54-story supplementally-damped buildings, respectively. Damping ratio of the component is assumed to be 3%. For the 29-story building (Fig. 24a) seismically-resistant, the curve of the broken line is generated from the floor acceleration record, and solid line is generated from floor accelerations that come from the modal superposition time-history analysis by assuming increased damping ratio of 4% for the first three modes. In contrast, for the three supplementally-damped buildings (Fig. 24b-d), the solid line is generated from the top floor acceleration records, and the broken line from floor accelerations that come from the time-history analysis by assuming decreased damping ratio of 1% for the first three modes. The plots indicate a merit of increasing building damping for protecting the acceleration-sensitive components.

According to Figure 24, the past belief that short-period components are safer in a tall building is incorrect. They are as vulnerable as the long-period components due to multiple resonance peaks created by different modes of the building. The peaks are extremely high,

even greater than  $2,000 \text{ cm/s}^2$  ( $\approx 2G$ ). Thus, the resonant acceleration of the components may be greater than  $8G$  at a so-called major quake 4 times or stronger. The problem may become more serious when damage and softening of components cause period shifting from one resonance peak to others. Note that three peaks for each building are shown in Figure 24, since the first three modes were identified. But more peaks may emerge in an actual low damping case.

As a rule of thumb, facilities may overturn when floor acceleration exceeds  $0.3G$ , and ceiling whose vibration period typically ranges from  $0.3$  to  $1\text{s}$  may fall when its acceleration response exceeds  $1G$ . These indicate the needs for an immediate attention to component responses at a major quake that will occur in Tokyo. Figure 24 also clearly indicates that even moderately increasing the building damping ratio by  $3\%$  or so would reduce the component acceleration considerably.

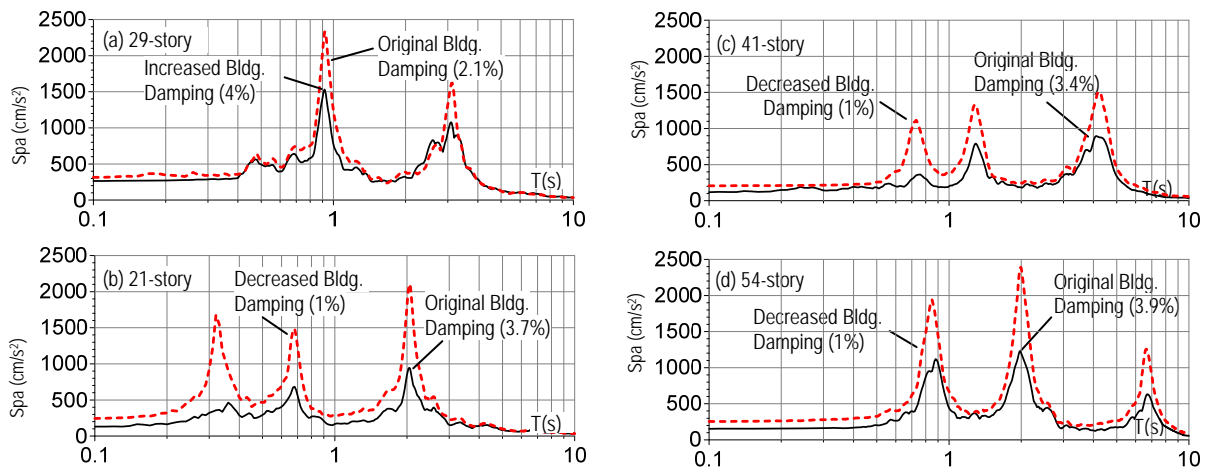


Figure 24. Component Response Spectra (Component Damping Ratio = 3%) at top floors of a seismically resistant building and three supplementally-damped buildings..

Finally, the solid line of Figure 25 shows the CAS at the top floor of the base-isolated 20-story building discussed above. It is generated from the floor acceleration record, and broken line is generated from floor accelerations that come from the modal superposition time-history analysis assuming the seismically-resistant building with no isolation system. Unlike Figure 24, the resonance period as well as the peak CAS values of the two buildings are very different, and good performance of the base-isolated building for acceleration control is clearly seen.

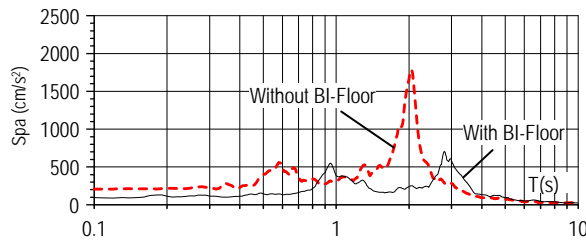


Figure 25. Component Response Spectra (Component Damping Ratio = 3%) at top floor of a base-isolated 20-story building

### Conclusions

Responses of the tall buildings in Tokyo during the 2011 Tohoku Earthquake are discussed based on the strong motions recorded. By successfully analyzing contributions of multiple vibration modes, various shaking phenomena in the tall building that had not been experienced are clarified. Moreover, the most significant evidence of response-control effectiveness was presented, and the merits of damping technology as well as base-isolation technology for occupants and contents are explained.

In most seismically-resistant tall buildings of steel construction, the damping ratios were approximately in the range between 0.01 and 0.02. This is believed to be a main reason for higher magnification of acceleration. Excessive accelerations have been found to cause large economic loss due to the damage on non-structural components and facilities. Thus, acceleration magnification should be taken in structural design more seriously.

The tall buildings with velocity dependent dampers had damping ratios of 0.03 to 0.05 typically. Their responses were compared with those generated from hypothetical analyses assuming low damping ratio of 0.01. They show reduction of peak responses, significantly faster decay of vibration, which would lead to reducing damage and fatigue of structural and non-structural components as well as fear of the occupants. In this regard, steel damper, although economical and effective for a major event, could be supplemented with velocity-dependent dampers for better performance.

In Kanto area, tall base-isolated buildings have shown for the first time the special vibration characteristics which had been expected but not observed until the 2011 Tohoku Earthquake. The loss of isolation effects due to slender configuration as well as moderate yielding and small energy dissipation of steel damper lead to magnification rather than reduction of the accelerations in the superstructure. For larger earthquake, the building performance is expected to be much better, but this point must be studied carefully.

Immediate attention must be given to mitigate acceleration-induced hazards in existing and new tall buildings against much stronger shaking likely to occur in the near future. The use of supplemental damping or base-isolation appears to be desirable, since it can reduce not only peak accelerations but also number of large response cycles, and duration of significant shaking.

The present paper has discussed issues related to response-control, focusing on global responses of the system. In order to assure such design, all members must be properly sized. Hence, designs for the components such as beams, columns, connections, and dampers are important and are currently studied by the writer and the colleagues.

References

- (1) Kasai, K., Motoyui, S., Ozaki, H., Ishii, M., Ito, H., Kajiwara, K., and Hikino, T. (2009), Full-Scale Tests of Passively-Controlled 5-Story Steel Building Using E-Defense Shake Table; Part 1 to Part 3, Proc. Stessa2009, Philadelphia.
- (2) Kasai, K. (2011a). 4.2.3 Acceleration records of buildings, 4.4.5. Behavior of response controlled buildings, Preliminary Reconnaissance Report of the 2011 Tohoku-Chiho Taiheiyō-Oki Earthquake, Architectural Institute of Japan, pp.280-284, pp.345-347.
- (3) Kasai, K. (2011b). Chapter 4. Performance of Response-Controlled Buildings, The Kenchiku Gijutsu, No.741, pp.118-123.
- (4) Hisada, Y., Kubo, T., and Yamashita, T. (2011), Shaking and Damage of the Shinjuku Campus Building and Shinjuku Campus Report from Kogakuin University, Internet Access: [http://kouzou.cc.kogakuin.ac.jp/Open/20110420Event/20Apr11\\_Kogakuin01.pdf](http://kouzou.cc.kogakuin.ac.jp/Open/20110420Event/20Apr11_Kogakuin01.pdf)
- (5) Koyama, S., and Kashima, T. (2011), Prompt Report on Strong Motions Recorded during the 2011 Tohoku Pacific Ocean Earthquake, Report 5, Building Research Institute (BRI).
- (6) Maseki, R., Nii, A., Nagashima, I., Aono, H., Kimura, Y., and Hosozawa, O. (2011), Performance of Seismic Retrofitting of Suoer High-Rise Building Based on Earthquake Observation Records, International Symposium on Disaster Simulation and Structural Safety in the Next Generation (DS'11), Japan
- (7) Isermann, R. and Münchhoff, M. (2011) Identification of Dynamic Systems: An Introduction with Applications, Springer, New York.
- (8) Hisada, Y., Yamashita, T., Murakami, M., Kubo, T., Shindo, J., Aizawa K., and Arata T. (2012), Seismic Response and Damage of High-Rise Buildings in Tokyo, Japan During the Great East Japan Earthquake, Proceedings, International Symposium on Engineering Lessons Learned from the Giant Earthquake, Tokyo, Japan, March 3 -4.
- (9) Kasai, K., Pu, W., and Wada, A. (2012): Responses of Tall Buildings in Tokyo during the 2011 Great East Japan Earthquake, Proc. of STESSA 2012 (Behaviour of steel structures in seismic areas), Keynote Paper, pp.25-35, Santiago, Chile, 9-11 January.
- (10) JSSI (2012), Japan Society of Seismic Isolation, "Report of Response-Controlled Buildings Investigation Committee," January 26, 2012, Tokyo, Japan.
- (11) Matsuda, K., Kasai, K., Yamagiwa, K., and Sato, D. (2012), Responses of Base-Isolated Buildings in Tokyo during the 2011 Great East Japan Earthquake, 15th WCEE, CD-ROM, Lisbon, Portugal, 2012.9
- (12) Kasai, K., Mita, K., Kitamura, H., Matsuda, K., Morgan, T., and Taylor, A. (2013), Performance of Seismic Protection Technologies During the 2011 Tohoku-Oki Earthquake, Earthquake Spectra, Special Issue on the 2011 Tohoku-Oki Earthquake and Tsunami, pp.265-294, 2013. 3
- (13) Kasai, K. (2013), Implications for Design of Response-Controlled Buildings from Full-Scale Lab Tests and Actual Earthquake Observations, 13th World Conference on Structural Control (13WCSI), Keynote Paper, Sendai, Japan, 2013.9

